scientific reports

Check for updates

OPEN

Mathematical analysis and molecular descriptors of two novel metal–organic models with chemical applications

Shahid Zaman[1], Mehwish Jalani[1], Asad Ullah[2], Wakeel Ahmad[1] & Ghulamullah Saeedi[3]✉

Metal–Organic Networks (MONs) are made by chemical molecules that contain metal ions and organic ligands. A crystalline porous solid called Metal–Organic Networks (MONs) is made up of a 3*D* metal network of ions held in place by a multidentate ligand. (MONs) can be used for gas storage, purification drug delivery, gas separation, catalysis, and sensing applications. There is enormous potential for effective integration and research of MONs in diverse applications. Molecular descriptors are arithmetic measures that reveal a chemical substance's physical and chemical characteristics in its foundational network in a natural relationship. They demonstrate an important role in theoretical and ecological chemistry, and in the field of medicine. In this research, we calculated various recently discovered molecular descriptors viz. the modified version of second zagreb index, harmonic index, reciprocal randic index, modified version of forgotten topological index, redefined first zagreb topological index, redefined second zagreb topological index and redefined third zagreb topological index for two separate metal–organic networks. The numerical and graphical comparative analysis of these considered molecular descriptors are also performed.

Every heavenly body is a combination of several constituents that significantly contributes to the composition of the earth. The three-element hydrogen, oxygen and nitrogen are the most significant ones on the planet[1,2]. Massively used compounds made by chemically like metal–organic network (MON) are thus made up of alloy ions/metallic ions and organic linkers. With the aid of the hydrothermal method, new MONs composed of zinc considered metal ions and benzene 1, 3-dicarboxylic acid as the organic linker[3]. Biography of MONs is their superficial alteration and as well as their particle control six division[4]. Devices with luminous properties could be created using *Zn*-related MONs, are chemical sensors[1]. In reality,Zn^{+2} an astringent, anti-dandruff, antibacterial, and anti-inflammatory autogenous simple powerless noxious conversion metal cation, is frequently worked in homoeopaths as a scarring catalyst and face ointment[5]. Additionally, the production processes of MONs related to zinc have lately been documented, and as well their toxicity, biological uses, and biocompatibility[6]. In modern chemistry, graph theory offers essential tools that depict chemical compounds' heats of formation, evaporation, flash points, temperatures, pressures, densities, and partition coefficients[7]. Zinc oxide is a white powder that is insoluble in water. Nanostructure of Zinc oxide (*Zno*) can be synthesized into a range of different morphologies. A variety of skin conditions can be treated with zinc oxide. In marine environments, zinc silicate coating can provide long-term protection of steel and is used in rapid coating work for over fifty years. Zinc oxide is also used in toothpastes to prevent plaque. These metals also help the human body, it is present in the red blood cells and causes several reactions related to carbon dioxide metabolism. Zinc silicate networks are economical because they are relatively thin coating.

The zinc oxide and zinc silicate exhibit physicochemical characteristics including grafting active groups[8], incorporating appropriate active material[9], ion exchange[10], creating composites using various materials[11], modifying organic ligands, photosynthetic ligands, and improving the selectivity, sensitivity, and response times of biosensors.Yap et al.[12] and Lin et al.[13] presented the most current developments in precursors for a variety of nanostructures and MON-related applications, including lithium ion batteries, super capacitors, photocatalysis, electrocatalysis, and catalysts for the manufacture of fine chemicals. The field of modern chemistry can benefit from using graph theory to represent the physical and chemical characteristics of chemical compounds, such as

[1]Department of Mathematics, University of Sialkot, Sialkot 51310, Pakistan. [2]Department of Mathematical Sciences, Karakoram International University Gilgit, Gilgit 15100, Pakistan. [3]Department of Mathematics, Polytechnical University of Kabul, Kabul, Afghanistan. ✉email: gh.saeedi@kpu.edu.af

their heats of formation and evaporation, flash points, melting points, boiling points, temperatures, pressures, densities, retention times in chromatography, tensions, and partition coefficients[14,15]. In order to investigate many characteristics of chemical compounds (such as the boiling point of paraffin), Wiener first developed the distance-based topological index (TI) in 1947. Gutman and Trinajsic's highly regarded first-degree-based TI was developed to test the chemical plausibility of the total π-electron energy of the chemical compounds (alternant hydrocar-bons).

The Zagreb type indices contributed tremendously in the various fields which can be seen in[16–21]. The details on other degree based molecular descriptors and structures are given in[22–27]. In 2021, the authors of[28] computed the connection-based Zagreb indices such as first Zagreb connection index (ZCI), second ZCI, modified first ZCI, modified second ZCI, modified third ZCI, and modified fourth ZCI. We extended those results for other degree based topological indices as Modified version of second Zagreb index $M_2(G)$, Harmonic index $H(G)$[29], Reciprocal Randic index $RR(G)$, the Modified version of Forgotten topological index F_N^*, the Redefined First Zagreb topological index $R_eZG_1(G)$[30], the Redefined Second Zagreb topological index $R_eZG_2(G)$[31] as well as the Redefined third Zagreb topological index $R_eZG_3(G)$[32] for MONs, namely Zinc oxide ($ZNOX(n)$) and zinc silicate ($ZNSL(n)$) as regards to the expanding layers,$n \geq 3$. Our outcomes fascinate not only mathematician but also of theoretical chemists. The results of this study can be used to examine numerical quantities and guide future research into the physical properties of molecules. As a consequence, it is a beneficial procedure to eliminate costly and time-consuming laboratory studies. The findings of this research depict that $R_eZG_3(G)$ achieved higher values than other classical Zagreb indices, which may have better correlation with the thirteen physicochemical characteristics of octane isomers.

Main results

Here, we initially present some significant definitions of the degree based molecular descriptors which will be useful to obtain the main results. In the whole study, we denote the adjacent vertices by p and q, i.e. $pq \in E_G$.

Definition 1 The molecular descriptor $M_2(G)$ denotes modified version of second zagreb index that is described as[33],

$$M_2(G) = \sum_{pq \in E(G)} \frac{1}{d_G(p) \times d_G(q)}$$

Definition 2 The molecular descriptor $H(G)$ denotes harmonic index which is defined in[34] as,

$$H(G) = \sum_{pq \in E(G)} \frac{2}{d_G(p) + d_G(q)}$$

Definition 3 The molecular descriptor $RR(G)$ denotes reciprocal randic index which is explained as[35],

$$RR(G) = \sum_{pq \in E(G)} \sqrt{d_G(p) \times d_G(q)}$$

Definition 4 The molecular descriptor F_N^* denotes modified version of forgotten topological index, that is described as[36],

$$F_N^*(G) = \sum_{pq \in E(G)} [d_G(p)^2 + d_G(q)^2]$$

Definition 5 The molecular descriptor R_eZG_1 denotes redefined first zagreb topological index, which is defined by[36],

$$R_eZG_1(G) = \sum_{pq \in E(G)} \frac{d_G(p) + d_G(q)}{d_G(p) \times d_G(q)}$$

Definition 6 The molecular descriptor $R_eZG_2(G)$ denotes the redefined second zagreb topological index, that is described as[31],

$$R_eZG_2(G) = \sum_{pq \in E(G)} \frac{d_G(p) \times d_G(q)}{d_G(p) + d_G(q)}$$

Definition 7 The molecular descriptor $R_eZG_3(G)$ denotes redefined third zagreb topological index, which is explained by[31],

$$R_eZG_3(G) = \sum_{pq \in E(G)} d_G(p) \times d_G(q)\left[d_G(p) + d_G(q)\right]$$

Theorem 1 *Let $H \cong ZNOX(n)$ is a zinc oxide network as depicted in Fig. 1, then*

$$M_2(G) = 11.928n + 9.7$$

Proof Based on the Definition 1 and Table 1, we have

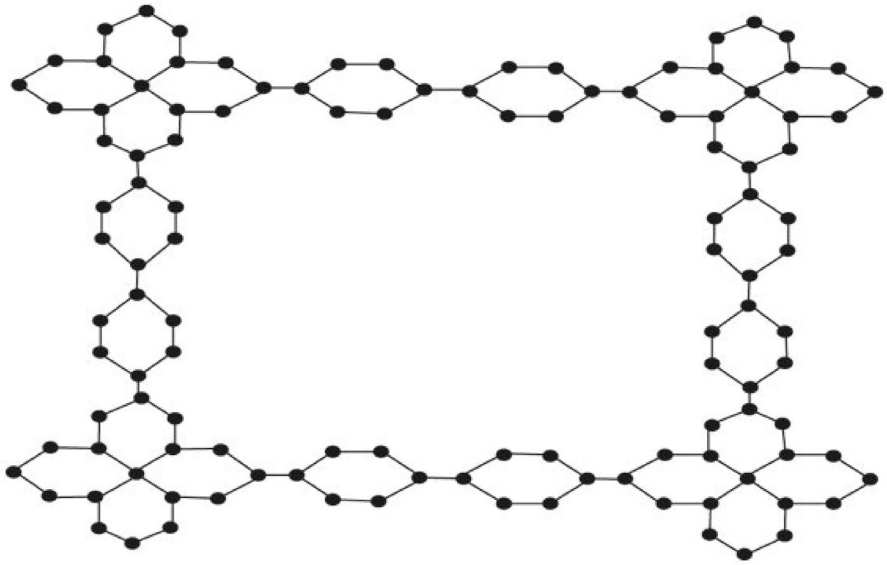

Figure 1. Zinc oxide network (ZNOX (n) $\cong$ H), where $n = 3$.

$E^d_{p,q}$	$E^d_{2,2}$	$E^d_{2,3}$	$E^d_{3,3}$	$E^d_{3,4}$
$\lvert E^d_{p,q}\rvert$	$6n+16$	$52n+28$	$9n+3$	$8n+8$

Table 1. Edge partition of *ZNOX* in relation to the degrees.

$$M_2(G) = \sum_{pq\in E(G)} \frac{1}{d_G(p)\times d_G(q)} = \sum_{pq\in E_{2,2}} \frac{1}{d_G(p)\times d_G(q)} + \sum_{pq\in E_{2,3}} \frac{1}{d_G(p)\times d_G(q)} + \sum_{pq\in E_{3,3}} \frac{1}{d_G(p)\times d_G(q)} + \sum_{pq\in E_{3,4}} \frac{1}{d_G(p)\times d_G(q)} = |E_{2,2}|\left(\frac{1}{2\times 2}\right) + |E_{2,3}|\left(\frac{1}{2\times 3}\right) + |E_{3,3}|\left(\frac{1}{3\times 3}\right) + |E_{3,4}|\left(\frac{1}{3\times 4}\right) = \frac{(6n+16)}{4} + \frac{(52n+28)}{6} + \frac{(9n+3)}{9} + \frac{(8n+8)}{12} M_2(G) = 11.928n + 9.7$$

Theorem 2 *Let $H \cong ZNOX(n)$ be a zinc oxide network as shown in Fig. 1, then*

$$H(G) = 29.01n + 22.43$$

Proof Based on the Definition 2 and Table 1, one has

$$H(G) = \sum_{pq\in E(G)} \frac{2}{d_G(p)+d_G(q)}$$
$$= |E_{2,2}|\left(\frac{2}{2+2}\right) + |E_{2,3}|\left(\frac{2}{2+3}\right) + |E_{3,3}|\left(\frac{2}{3+3}\right) + |E_{3,4}|\left(\frac{2}{3+4}\right)$$
$$= 3n + 8 + 20.8n + 11.2 + 2.97n + 0.99 + 2.24n + 2.24$$
$$H(G) = 29.01n + 22.43.$$

Theorem 3 *Let $H \cong ZNOX(n)$ be a zinc oxide network as shown in Fig. 1, then*

$$\mathrm{RR(G)} = 193.56\mathrm{n} + 137$$

Proof Based on the Definition 3 and Table 1, one has

$$RR(G) = \sum_{pq \in E(G)} \sqrt{d_G(p) \times d_G(q)}$$
$$= \sqrt{2 \times 2}|E_{2,2}| + \sqrt{2 \times 3}|E_{2,3}| + \sqrt{3 \times 3}|E_{3,3}| + \sqrt{3 \times 4}|E_{3,4}|$$
$$= \sqrt{4} \times (6n + 16) + \sqrt{6} \times (52n + 28) + \sqrt{9} \times (9n + 3) + \sqrt{12} \times (8n + 8)$$
$$\mathrm{RR(G)} = 193.56\mathrm{n} + 137$$

Theorem 4 *Let $H \cong ZNOX(n)$ be a zinc oxide network as shown in Fig. 1, then*

$$\mathrm{R_eZG_1(G)} = 59.97\mathrm{n} + 46$$

Proof Based on the Definition 5 and Table 1, we have

$$R_eZG_1(G) = \sum_{pq \in E(G)} \frac{d_G(p) + d_G(q)}{d_G(p) \times d_G(q)}$$
$$= \frac{2+2}{2 \times 2}|E_{2,2}| + \frac{2+3}{2 \times 3}|E_{2,3}| + \frac{3+3}{3 \times 3}|E_{3,3}| + \frac{3+4}{3 \times 4}|E_{3,4}|$$

$$\mathrm{R_eZG_1(G)} = 59.97n + 46$$

The following corollary is a direct consequent of Theorem 4.

Corollary 5 *Let $H \cong ZNOX(n)$ be a zinc oxide network as depicted in Fig. 1, then*

$$R_eZG_2(G) = 95.612n + 67.812$$

Theorem 6 *Let $H \cong ZNOX(n)$ be a zinc oxide network as shown in Fig. 1, then*

$$R_eZG_3(G) = 2814n + 1930$$

Proof Based on the Definition 7 and Table 1, we have

$$R_eZG_3(G) = \sum_{pq \in E(G)} d_G(p) \times d_G(q)[d_G(p) + d_G(q)]$$
$$= (2)(2)[2+2]|\mathrm{E}_{2,2}| + (2)(3)[2+3]|\mathrm{E}_{2,3}| + (3)(3)[3+3]|\mathrm{E}_{3,3}| + (3)(4)[3+4]|\mathrm{E}_{3,4}|$$
$$= 4(4)(6\mathrm{n} + 16) + 6(5)(52\mathrm{n} + 28) + 9(6)(9\mathrm{n} + 3) + (12)7(8\mathrm{n} + 8)$$

$$R_eZG_3(G) = 2814n + 1930$$

Theorem 7 *Let $H \cong ZNOX(n)$ be a zinc oxide network as depicted in Fig. 1, then*

$$F_N^*(G) = 1086n + 746$$

Proof Based on the Definition 4 and Table 1, one has

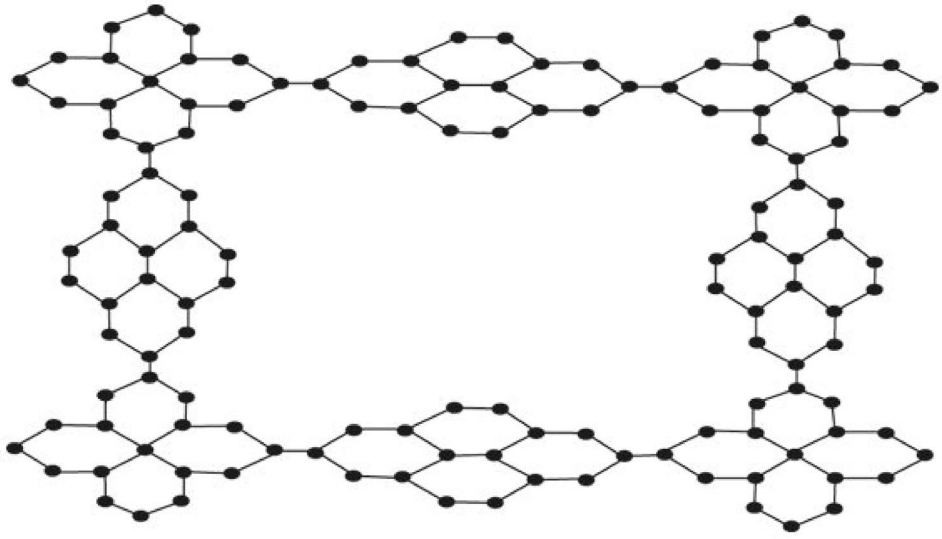

Figure 2. Zinc silicate network (ZNSL (n) $\cong$ K), where $n = 3$.

$E^d_{p,q}$	$E^d_{2,2}$	$E^d_{2,3}$	$E^d_{3,3}$	$E^d_{3,4}$
$\lvert E^d_{p,q}\rvert$	$10n+14$	$64n+32$	$21n+7$	$8n+8$

Table 2. Edge partition of *ZNSL* in relation to the degrees.

$$F_N^*(G) = \sum_{pq\in E(G)}[d_G(p)^2 + d_G(q)^2] = \sum_{pq\in E(2,2)}[d_G(p)^2 + d_G(q)^2] + \sum_{pq\in E(2,3)}[d_G(p)^2 + d_G(q)^2] + \sum_{pq\in E(3,3)}[d_G(p)^2 + d_G(q)^2] + \sum_{pq\in E(3,4)}[d_G(p)^2 + d_G(q)^2]$$

$$F_N^*(G) = 1086n + 746$$

Theorem 8 *Suppose $K \cong ZNSL(n)$ be a zinc silicate network as depicted by Fig. 2, then*

$$M_2(G) = 16.17n + 10.28$$

Proof Based on the Definition 1 and Table 2, we have

$$M_2(G) = \sum_{pq\in E(G)} \frac{1}{d_G(p)\times d_G(q)}$$
$$= \sum_{pq\in E_{2,2}} \frac{1}{d_G(p)\times d_G(q)} + \sum_{pq\in E_{2,3}} \frac{1}{d_G(p)\times d_G(q)} + \sum_{pq\in E_{3,3}} \frac{1}{d_G(p)\times d_G(q)} + \sum_{pq\in E_{3,4}} \frac{1}{d_G(p)\times d_G(q)}$$
$$= |E_{2,2}|\left(\frac{1}{2\times 2}\right) + |E_{2,3}|\left(\frac{1}{2\times 3}\right) + |E_{3,3}|\left(\frac{1}{3\times 3}\right) + |E_{3,4}|\left(\frac{1}{3\times 4}\right)$$

$$M_2(G) = 16.17n + 10.28$$

Theorem 9. *Suppose $K \cong ZNSL(n)$ be a zinc silicate network as shown by Fig. 2, then*

$$H(G) = 39.88n + 24.41$$

Proof Based on the Definition 2 and Table 2, we have

$$H(G) = \sum_{pq\in E(G)} \frac{2}{d_G(p)+d_G(q)}$$
$$= \sum_{pq\in E(2,2)} \frac{2}{d_G(p)+d_G(q)} + \sum_{pq\in E(2,3)} \frac{2}{d_G(p)+d_G(q)} + \sum_{pq\in E(3,3)} \frac{2}{d_G(p)+d_G(q)} + \sum_{pq\in E(3,4)} \frac{2}{d_G(p)+d_G(q)}$$
$$= |E_{2,2}|\left(\frac{2}{2+2}\right) + |E_{2,3}|\left(\frac{2}{2+3}\right) + |E_{3,3}|\left(\frac{2}{3+3}\right) + |E_{3,4}|\left(\frac{2}{3+4}\right)$$

$$H(G) = 39.88n + 24.41$$

Theorem 10 *Suppose $K \cong ZNSL(n)$ be a zinc silicate network as shown by Fig. 2, then*

$$RR(G) = 266.84n + 154.76$$

Proof Based on the Definition 3 and Table 2, one has

$$\mathrm{RR(G)} = \sum_{pq\in E(G)} \sqrt{d_G(p)\times d_G(q)}$$
$$= \sqrt{2\times 2}|E_{2,2}| + \sqrt{2\times 3}|E_{2,3}| + \sqrt{3\times 3}|E_{3,3}| + \sqrt{3\times 4}|E_{3,4}|$$
$$= \sqrt{4}(10n+14) + \sqrt{6}(64n+32) + \sqrt{9}(21n+7) + \sqrt{12}(8n+8)$$

$$\mathrm{RR(G)} = 266.84\mathrm{n} + 154.76$$

Theorem 11 *Suppose $K \cong ZNSL(n)$ be a zinc silicate network as depicted by Fig. 2,*

$$R_eZG_1(G) = 82n + 50.01$$

Proof Based on the Definition 5 and Table 2, one has

$$\mathrm{R_eZG_1(G)} = \sum_{pq\in E(G)} \frac{d_G(p)+d_G(q)}{d_G(p)\times d_G(q)}$$
$$= \frac{2+2}{2\times 2}|E_{2,2}| + \frac{2+3}{2\times 3}|E_{2,3}| + \frac{3+3}{3\times 3}|E_{3,3}| + \frac{3+4}{3\times 4}|E_{3,4}|$$

$$\mathrm{R_eZG_1(G)} = 82n + 50.01$$

The following corollary is a direct consequent of Theorem 11.

Corollary 12 *Suppose $K \cong ZNSL(n)$ be a zinc silicate network as shown by Fig. 2, then*

$$R_eZG_2(G) = 132.01\mathrm{n} + 76.61$$

Theorem 13 *Suppose $K \cong ZNSL(n)$ be a zinc silicate network as shown by Fig. 2, then*

$$R_eZG_3(G) = 3886n + 2234$$

Proof Based on the Definition 7 and Table 2, one has

$$R_eZG_3(G) = \sum_{pq\in E(G)} d_G(p)\times d_G(q)\left[d_G(p)+d_G(q)\right]$$
$$= (2)(2)[2+2]\left|\mathrm{E}_{2,2}\right| + (2)(3)[2+3]\left|\mathrm{E}_{2,3}\right| + (3)(3)[3+3]\left|\mathrm{E}_{3,3}\right| + (3)(4)[3+4]\left|\mathrm{E}_{3,4}\right|$$
$$= 4(4)(10\mathrm{n}+14) + 6(5)(64\mathrm{n}+32) + 9(6)(21\mathrm{n}+7) + (12)7(8\mathrm{n}+8)$$

$$R_eZG_3(G) = 3886n + 2234$$

Theorem 14 *Suppose $K \cong ZNSL(n)$ be a zinc silicate network as shown by Fig. 2, then*

$$\mathrm{F_N^*(G)} = 1490\mathrm{n} + 854$$

Proof Considering Table 2 and Definition 4, we can write

$$F_N^*(G) = \sum_{pq\in E(G)} [d_G(p)^2 + d_G(q)^2]$$
$$= \sum_{pq\in E(2,2)} [d_G(p)^2 + d_G(q)^2] + \sum_{pq\in E(2,3)} [d_G(p)^2 + d_G(q)^2]$$
$$+ \sum_{pq\in E(3,3)} [d_G(p)^2 + d_G(q)^2] + \sum_{pq\in E(3,4)} [d_G(p)^2 + d_G(q)^2]$$
$$= [8](10n+14) + [13](64n+32) + [18](21n+7) + [25](8n+8)$$

$$F_N^*(G) = 1490n + 85$$

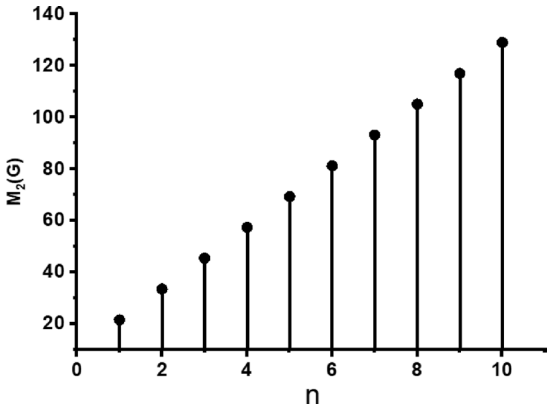

Figure 3. The comparison of n and $M_2(G)$.

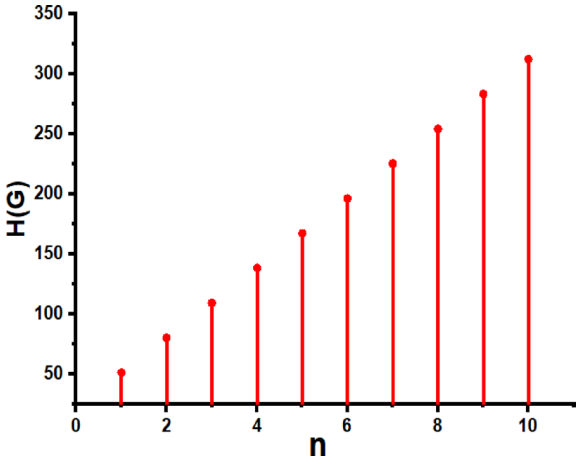

Figure 4. The comparison of n and $.H(G)$

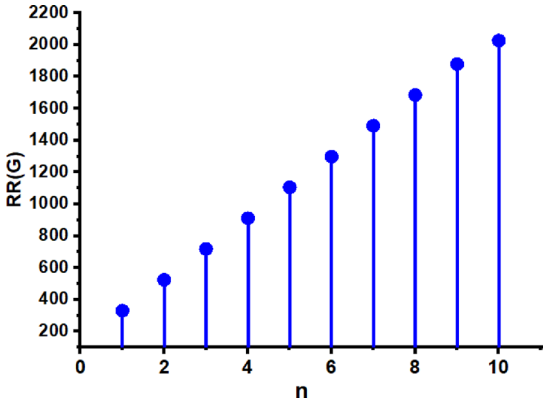

Figure 5. The comparison of n and $.RR(G)$

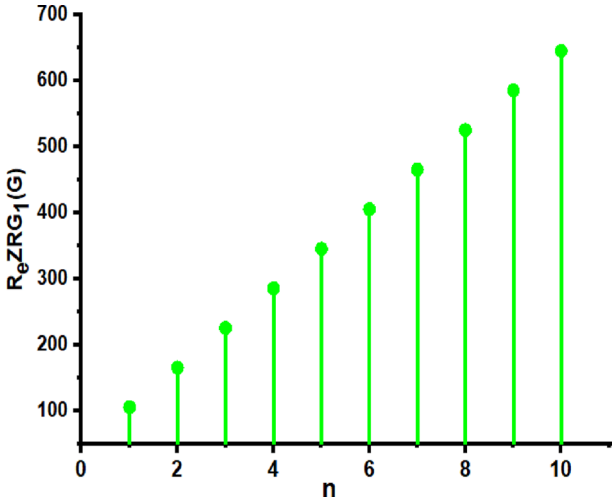

Figure 6. The comparison of n and $.R_eZRG_1(G)$

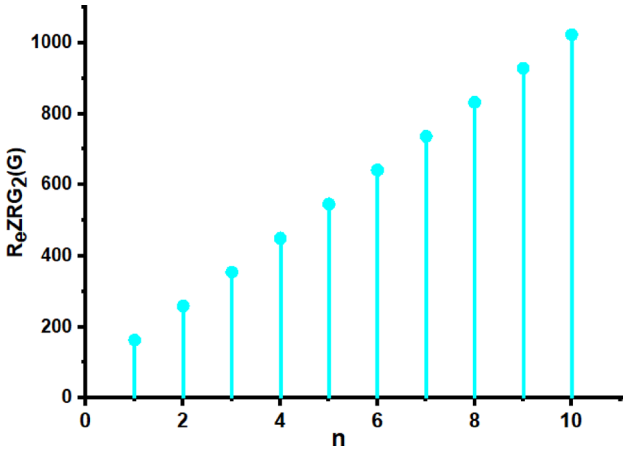

Figure 7. The comparison of n and $.R_eZRG_2(G)$

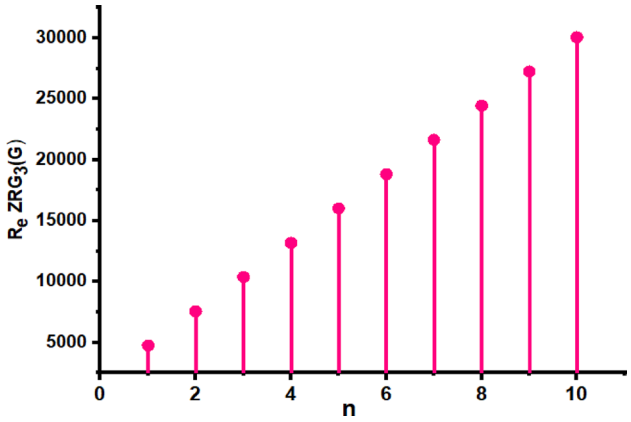

Figure 8. The comparison of n and $.R_eZRG_3(G)$

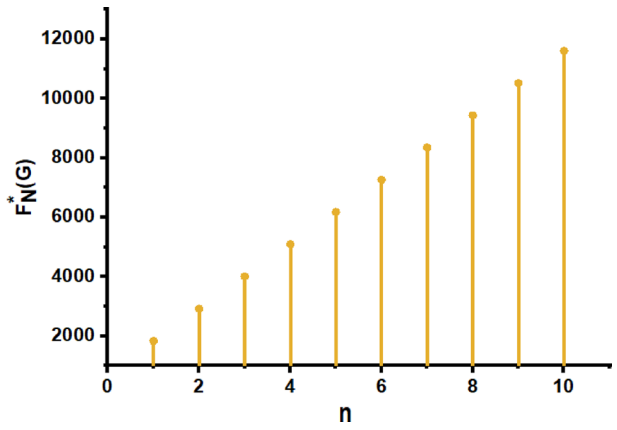

Figure 9. The comparison of n and $F_N^*(G)$.

Graphical interpretations

In this part, we worked out all indices numerically and presented the results in the table below. From Figs. 3, 4, 5, 6, 7, 8, 9 and Table 3, it is easy to see a positive relationship between n and the considered topological indices. As we increase n, the topological indices also increase. The comparative graphs of $M_2(G)$, $H(G)$, $RR(G)$, $R_eZG_1(G)$, $R_eZG_2(G)$, $R_eZG_3(G)$ and $F_N^*(G)$ indices of ZNOX for various values are presented in Fig. 10. Thus, Fig. 10 describe that all indices for ZNOX increase for increasing value of n. The increasing rate of $R_eZG_3(G)$ is higher than that of other topological indices. This depict that, $R_eZG_3(G)$ achieved higher values than other

[n]	$M_2(G)$	$H(G)$	$RR(G)$	$R_eZG_1(G)$	$R_eZG_2(G)$	$R_eZG_3(G)$	$F_N^*(G)$
[1]	21.628	51.44	330.56	105.94	163.424	4744	1832
[2]	33.556	80.45	524.12	165.94	259.034	7558	2918
[3]	45.484	109.46	717.68	225.91	354.648	10, 372	4004
[4]	57.412	138.47	911.24	285.88	450.26	13, 186	5090
[5]	69.34	167.48	1104.8	345.85	545.872	16, 000	6176
[6]	81.268	196.49	1298.36	405.82	641.484	18, 814	7262
[7]	93.196	225.5	1491.9	465.79	737.096	21, 628	8348
[8]	105.124	254.51	1685.4	525.76	832.708	24, 442	9434
[9]	117.052	283.52	1879.04	585.73	928.32	27, 256	10, 520
[10]	128.98	312.53	2027.6	645.7	1023.93	30, 070	11, 606

Table 3. Comparison of $M_2(G)$, $H(G)$, $RR(G)$, $R_eZG_1(G)$, $R_eZG_2(G)$, $R_eZG_3(G)$ and $F_N^*(G)$ for ZNOX.

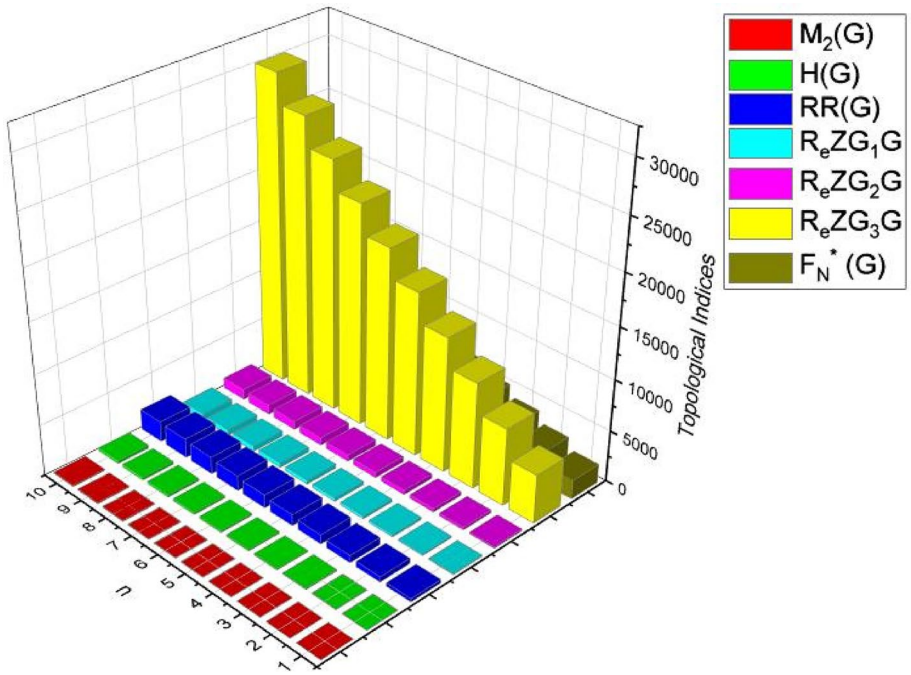

Figure 10. Comparison of topological indices for various values of n in ZNOX.

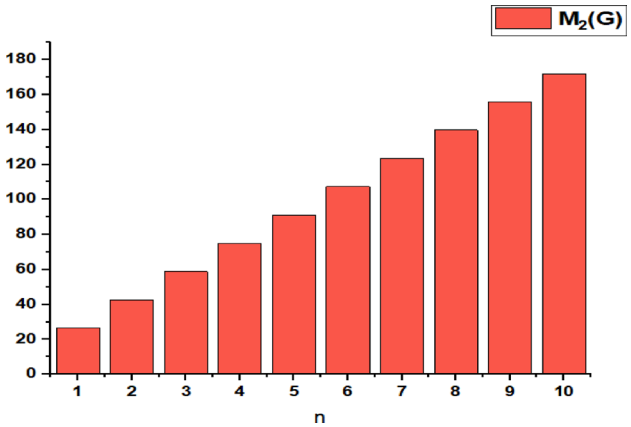

Figure 11. The comparison of n and $M_2(G)$.

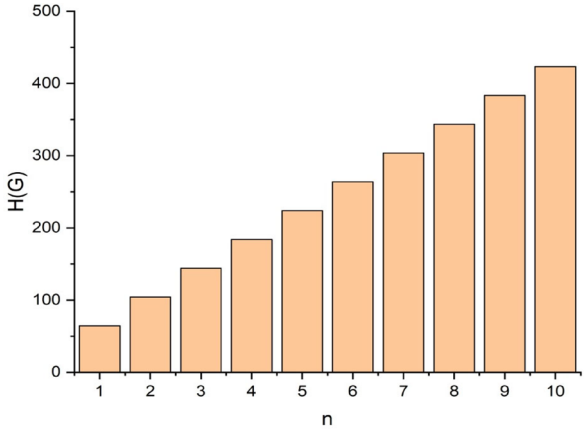

Figure 12. The comparison of n and $.H(G)$

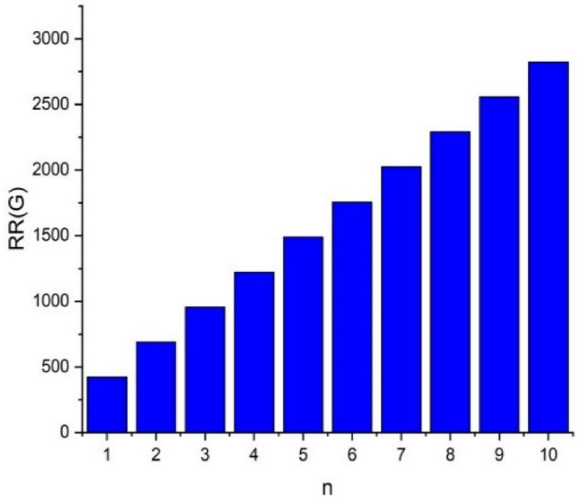

Figure 13. The comparison of n and $.RR(G)$

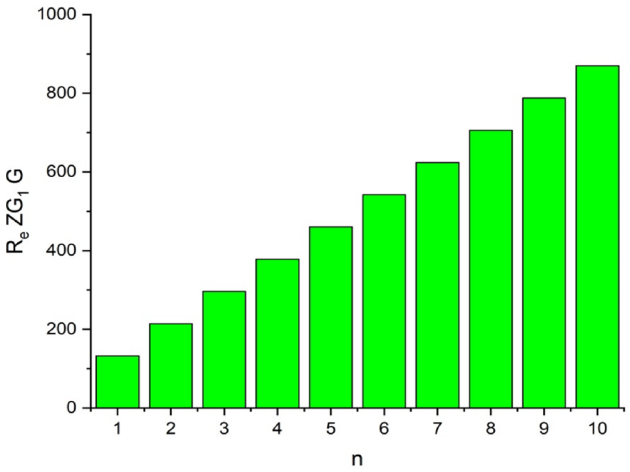

Figure 14. The comparison of n and $.R_eZG_1(G)$

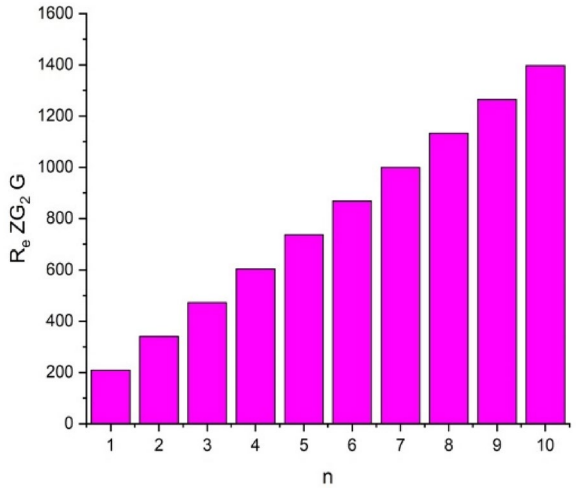

Figure 15. The comparison of n and .$R_eZG_2(G)$

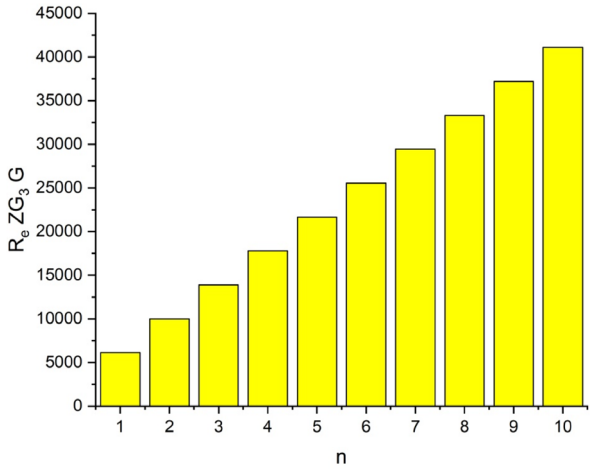

Figure 16. The comparison of n and .$R_eZG_3(G)$

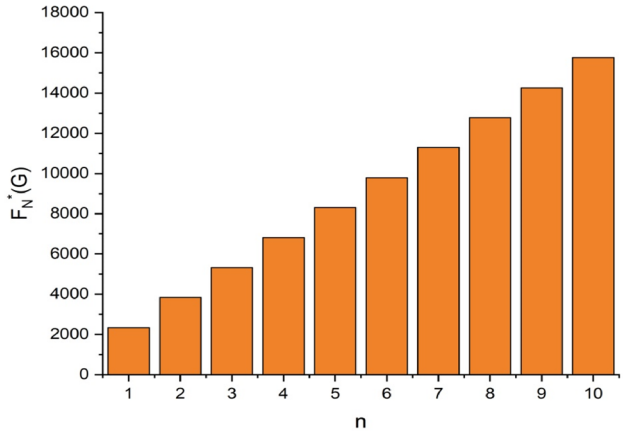

Figure 17. The comparison of n and $F_N^*(G)$.

[n]	$M_2(G)$	$H(G)$	$RR(G)$	$R_eZG_1(G)$	$R_eZG_2(G)$	$R_eZG_3(G)$	$F_N^*(G)$
[1]	26.45	64.29	421.6	132.01	208.62	6120	2344
[2]	42.62	104.17	688.44	214.01	340.63	10, 006	3834
[3]	58.79	144.05	955.28	296.01	472.64	13, 892	5324
[4]	74.96	183.93	1222.12	378.01	604.65	17, 778	6814
[5]	91.13	223.81	1488.96	460.01	736.66	21, 664	8304
[6]	107.3	263.69	1755.8	542.01	868.67	25, 550	9794
[7]	123.47	303.57	2022.6	624.01	1000	29, 436	11, 284
[8]	139.64	343.45	2289.4	706.01	1132.6	33, 322	12, 774
[9]	155.81	383.33	2556.3	788.01	1264.7	37, 208	14, 264
[10]	171.98	423.21	2823.1	870.01	1396.71	41, 094	15, 754

Table 4. Comparison of $M_2(G)$, $H(G)$, $RR(G)$, $R_eZG_1(G)$, $R_eZG_2(G)$, $R_eZG_3(G)$ and $F_N^*(G)$.

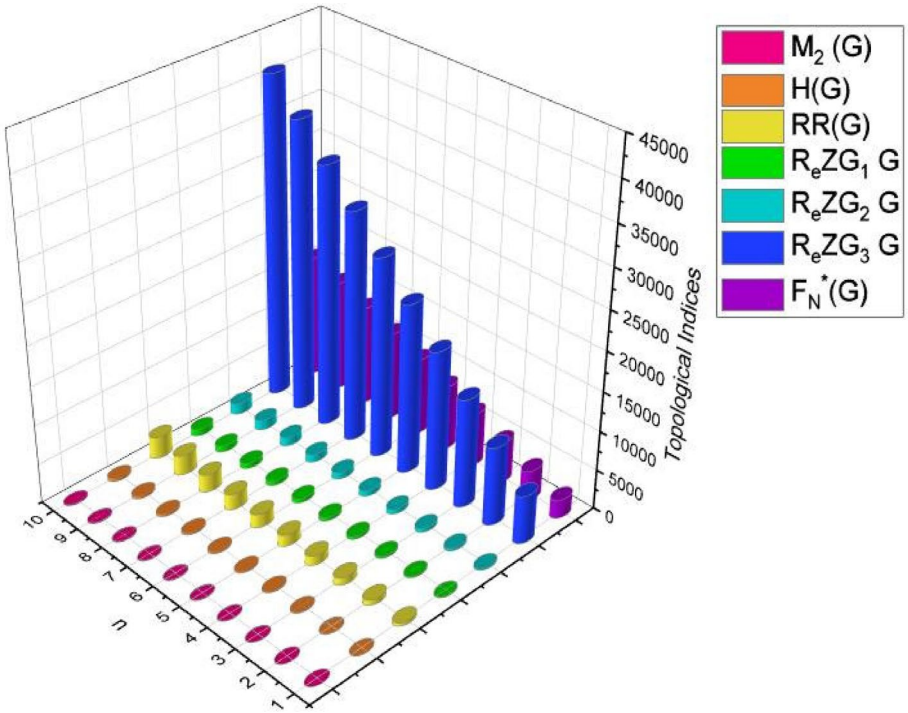

Figure 18. Comparison of topological indices for various values of n in $ZNSL$.

classical Zagreb indices, which may have better correlation with the thirteen physicochemical characteristics of octane isomers.

From Figs. 11, 12, 13, 14, 15, 16, 17 and Table 4, it is easy to see a positive relationship between n and the considered topological indices. As we increase n, the topological indices also increase. Meanwhile, the comparative relationship of $M_2(G)$, $H(G)$, $RR(G)$, $R_eZG_1(G)$, $R_eZG_2(G)$, $R_eZG_3(G)$ and $F_N^*(G)$ indices of $ZNSL$ for various values are presented in Fig. 18. Thus, Fig. 18 describe that all indices for ZNOX increase for increasing value of n. The increasing rate of $R_eZG_3(G)$ is higher than that of other topological indices. This depicts that, $R_eZG_3(G)$ achieved higher values than other classical Zagreb indices, which may have better correlation with the thirteen physicochemical characteristics of octane isomers.

Conclusion

In this research, we calculated various recently discovered molecular descriptors for two separate metal–organic networks. The molecular descriptors which we considered are $M_2(G)$, $H(G)$, $RR(G)$, $F_N^*(G)$, $R_eZG_1(G)$, $R_eZG_2(G)$ as well as $R_eZG_3(G)$. The two metal–organic networks we considered are, Zinc oxide ($ZNOX(n)$) and zinc silicate ($ZNSL(n)$). The numerical and graphical comparative analysis of the considered molecular descriptors are also performed. The obtained results depict that $R_eZG_3(G)$ achieved higher values than other classical Zagreb indices, which may have better correlation with the thirteen physicochemical characteristics of octane isomers.

It is quite motivating to study the distance based topological indices for the Metal–Organic Networks. In the near future we will carry it out.

Data availability

All data generated or analysed during this study are included in this article.

Received: 27 October 2022; Accepted: 26 March 2023
Published online: 31 March 2023

References

1. Yin, Z. *et al.* Synergistic stimulation of metal–organic frameworks for stable super-cooled liquid and quenched glass. *J. Am. Chem. Soc.* **144**, 13021–13025 (2022).
2. Petit, C. & Bandosz, T. J. MOF–graphite oxide nanocomposites: surface characterization and evaluation as adsorbents of ammonia. *J. Mater. Chem.* **19**, 6521–6528 (2009).
3. Kowsura, C., Pangkumhang, B., Jutaporn, P. & Tanboonchuy, V. Isotherm models of heavy metal sorption onto zinc-tricarboxylic. *Int. J. Chem. Eng. Appl.* **8**, 179–183 (2017).
4. Ibrahim, M. *et al.* Facile ultrasound-triggered release of calcein and doxorubicin from iron-based metal-organic frameworks. *J. Biomed. Nanotechnol.* **16**, 1359–1369 (2020).
5. Cui, Y. *et al.* A luminescent mixed-lanthanide metal–organic framework thermometer. *J. Am. Chem. Soc.* **134**, 3979–3982 (2012).
6. Prasad, A. S. Zinc in human health: effect of zinc on immune cells. *Mol. Med.* **14**, 353–357 (2008).
7. Bahrani, S., Hashemi, S. A., Mousavi, S. M. & Azhdari, R. Zinc-based metal–organic frameworks as nontoxic and biodegradable platforms for biomedical applications: Review study. *Drug Metab. Rev.* **51**, 356–377 (2019).
8. Hwang, Y. K. *et al.* Amine grafting on coordinatively unsaturated metal centers of MOFs: consequences for catalysis and metal encapsulation. *Angew. Chem. Int. Ed.* **120**, 4212–4216 (2008).
9. Thornton, A. W., Nairn, K. M., Hill, J. M., Hill, A. J. & Hill, M. R. Metal– organic frameworks impregnated with magnesium-decorated fullerenes for methane and hydrogen storage. *J. Am. Chem. Soc.* **131**, 10662–10669 (2009).
10. Kim, M., Cahill, J. F., Fei, H., Prather, K. A. & Cohen, S. M. Postsynthetic ligand and cation exchange in robust metal–organic frameworks. *J. Am. Chem. Soc.* **134**, 18082–18088 (2012).
11. Ahmed, I. & Jhung, S. H. Composites of metal–organic frameworks: preparation and application in adsorption. *Mater. Today* **17**, 136–146 (2014).
12. Yap, M. H., Fow, K. L. & Chen, G. Z. Synthesis and applications of MOF-derived porous nanostructures. *Green Energy Environ.* **2**, 218–245 (2017).
13. Lin, R.-B., Xiang, S., Xing, H., Zhou, W. & Chen, B. Exploration of porous metal–organic frameworks for gas separation and purification. *Coord. Chem. Rev.* **378**, 87–103 (2019).
14. Ullah, A., Udin, S., Zaman, S. & Humraz, A. Zagreb connection topological descriptors and structural property of the triangular chain structures. *Phys. Script* **1**, 1 (2023).
15. Zaman, S., Jalani, M., Ullah, A., Ali, M. & Shahzadi, T. On the topological descriptors and structural analysis of cerium oxide nanostructures. *Chem. Papers DO* **I**, 1–6 (2023).
16. Gutman, I. Selected properties of the Schultz molecular topological index. *J. Chem. Inf. Comput. Sci.* **34**, 1087–1089 (1994).
17. Zaman, S., Jalani, M., Ullah, A. & Saeedi, G. Structural analysis and topological characterization of sudoku nanosheet. *J. Math.* **1**, 1 (2022).
18. Ashrafi, A., Eliasi, M. & Ghalavand, A. Laplacian coefficients and Zagreb indices of trees. *Linear Multilinear Algebra* **67**, 1736–1749 (2019).
19. Zaman, S., Koam, A. N., Khabyah, A. & Ahmad, A. The kemeny's constant and spanning trees of hexagonal ring network. *Comput. Mater. Con.* **73**, 6347–6365 (2022).
20. Aslam, A., Nadeem, M. F., Zahid, Z., Zafar, S. & Gao, W. Computing certain topological indices of the line graphs of subdivision graphs of some rooted product graphs. *Mathematics* **7**, 393 (2019).
21. Khabyah, A. A., Zaman, S., Koam, A. N., Ahmad, A. & Ullah, A. Minimum zagreb eccentricity indices of two-mode network with applications in boiling point and benzenoid hydrocarbons. *Mathematics* **10**, 1393 (2022).
22. Ullah, A., Qasim, M., Zaman, S. & Khan, A. Computational and comparative aspects of two carbon nanosheets with respect to some novel topological indices. *Ain Shams Eng. J.* **13**, 101672 (2022).
23. Zaman, S. Cacti with maximal general sum-connectivity index. *J. Appl. Math. Comput.* **65**, 147–160 (2021).
24. Ullah, A., Zeb, A. & Zaman, S. A new perspective on the modeling and topological characterization of H-Naphtalenic nanosheets with applications. *J. Mol. Model.* **28**, 211 (2022).
25. Ullah, A., Shamsudin, S., Zaman, S., Hamraz, A. & Saeedi, G. Network-based modeling of the molecular topology of fuchsine acid dye with respect to some irregular molecular descriptors. *J. Chem.* **813**, 1276 (2022).
26. Zaman, S., & Ullah, A. Kemeny's constant and global mean first passage time of random walks on octagonal cell network. *Math. Methods Appl. Sci.* (2023).
27. Yu, X., Zaman, S., Ullah, A., Saeedi, G. & Zhang, X. Matrix analysis of hexagonal model and its applications in global mean-first-passage time of random walks. *IEEE Access* **11**, 10045–10052 (2023).
28. Hussain, M. T., Javaid, M., Ali, U., Raza, A. & Alam, M. N. Comparing zinc oxide-and zinc silicate-related metal-organic networks via connection-based Zagreb indices. *J. Chem.* **2021**, 1–16 (2021).
29. Du, Z., Ali, A. & Trinajstić, N. Alkanes with the first three maximal/minimal modified first Zagreb connection indices. *Mol. Inf.* **38**, 1800116 (2019).
30. Zhong, L. The harmonic index for graphs. *Appl. Math. Lett.* **25**, 561–566 (2012).
31. Shanmukha, M., Basavarajappa, N., Usha, A. & Shilpa, K. Novel neighbourhood redefined first and second Zagreb indices on carborundum structures. *J. Appl. Math. Comput.* **66**, 263–276 (2021).
32. Alameri, A., Shubatah, M. & Alsharafi, M. Zagreb indices, Hyper Zagreb indices and Redefined Zagreb indices of conical graph. *Adv. Math. Sci. J.* **9**, 3631–3642 (2020).
33. Shanmukha, M., Usha, A., Basavarajappa, N., Savitha, K. & Shilpa, K. A general neighborhood redefined Zagreb index on Boron Nanotubes. *Malay. J. Mat.* **9**, 836–843 (2021).
34. Li, S., Shi, L. & Gao, W. Two modified Zagreb indices for random structures, main group metal. *Chemistry* **44**, 150–156 (2021).
35. Li, Y.-X., Rauf, A., Naeem, M., Binyamin, M. A. & Aslam, A. Valency-based topological properties of linear hexagonal chain and hammer-like benzenoid. *Complexity* **2021**, 1–16 (2021).
36. Furtula, B. & Gutman, I. A forgotten topological index. *J. Math. Chem.* **53**, 1184–1190 (2015).

Author contributions

All have equally subsidized to this paper in all steps, from conceptualization to the write-up of final draft. All authors have approved the manuscript and given consent for publication.

Funding

The author Asad Ullah gratefully acknowledge the financial support for this study derived from the Higher Education Commission of Pakistan (Grant No. 20–11682/NRPU/R&D/HEC/2020).

Competing interests

The authors declare no competing interests.

Additional information

Correspondence and requests for materials should be addressed to G.S.

Reprints and permissions information is available at www.nature.com/reprints.

Publisher's note Springer Nature remains neutral with regard to jurisdictional claims in published maps and institutional affiliations.